Supplementary Information

Fluorescent indicator displacement assay for discovery of UGGAA repeat-targeted small molecules

Tomonori Shibata,*[a] Yasumasa Matsumoto,[b] Akiko Iihara,[b] Kazunori Yamada,[b] Hiroshi Ochiai,[b] Ryo Saito,[b] Shinichi Kusaka,[b] and Toshiyuki Kume,[b]

[a] Department of Regulatory Bioorganic Chemistry, *SANKEN (The Institute of Scientific and Industrial Research), Osaka University, 8-1 Mihogaoka, Ibaraki 567-0047, Japan*
[b] Sohyaku. Innovative Research Division, Mitsubishi Tanabe Pharma Corporation, 1-1-1, Marunouchi, Chiyoda-ku, Tokyo 100-8205, Japan

Contents

Experimental section

***T_m* measurements:** Thermal denaturation profiles were recorded on a UV-2700 spectrophotometer (Shimadzu) equipped with a TMSPC-8 temperature controller and a 10 mm path-length cell. The absorbance of r(UGGAA)$_9$ (2 μM) without and with ligand (20 or 40 μM) in sodium phosphate buffer (10 mM, pH 7.0) containing NaCl (100 mM) was monitored at 260 nm from 2 to 100 °C (1 °C min^{-1}). T_m was calculated by using the median method.

CSI-TOF-MS measurements: Samples were prepared by mixing r(UGGAA)$_5$ (10 μM) and NBD-NCD (50 or 100 μM) in 50% methanol in water containing 100 mM ammonium acetate. Mass spectra were obtained with JEOL JMS-T100LP AccuTOF LC-plus 4G mass spectrometer in negative mode. The spray temperature was fixed at –10 °C with a sample flow rate of 20 μL min^{-1}.

CD measurements: CD experiments were carried out on a J-725 CD spectrometer (JASCO) using a 10 mm path-length cell. CD spectra of 2 μM r(UGGAA)$_9$ in the absence and presence of NBD-NCD (20 μM) were measured in sodium phosphate buffer (10 mM, pH 7.0) containing NaCl (100 mM).

RNA titration experiments: RNA titration experiments were performed with a mixture of r(UGGAA)$_n$ (50, 100, 200, 400 nM) and NBD-NCD (1 μM) in sodium phosphate buffer (10 mM, pH 7.0) containing 1% DMSO, 0.1% Triton-X, and NaCl (100 mM) at room temperature. The fluorescence intensity (FI) and fluorescence polarization (FP) were measured with 490 nm excitation and 540 nm emission using a microplate reader (Spark). The normalized FI was calculated by normalization with the FI of only NBD.

FID assay: The FID assay was performed with a mixture of r(UGGAA)$_9$ (200 nM), NBD-NCD (1 μM), and ligand (10 μM) in sodium phosphate buffer (10 mM, pH 7.0) containing 1% DMSO, 0.1% Triton-X, and NaCl (100 mM) at room temperature using a microplate reader (Spark). In ligand titration experiments, ligand concentration was 1–20 μM. The FI of each well containing sample (100 μL for 96-well plate or 20 μL for 384-well plate) was measured with 490 nm excitation and 540 nm emission. In the FID assay for SMN-C5, risdiplam, CM-D1, and CM-D2, the fluorescence readings were taken with 510 nm excitation and 560 nm emission. The fold

change in FI was calculated by normalization with the FI of NBD-NCD with r(UGGAA)$_9$. In Fig. 4c, the FI of NBD-NCD with r(UGGAA)$_9$ and ligand was subtracted from the FI of only ligand and then was normalized with FI of NBD-NCD with r(UGGAA)$_9$.

Surface plasmon resonance (SPR) assay

5'-biotin-TEG r(UGGAA)$_9$ was immobilized on the SA sensor chip (BIAcore) that coated the surface with streptavidin. The surface of sensor chip SA was washed with 50 mM NaOH and 1 M NaCl at three times for 60 s with the flow rate of 30 μl min^{-1}. 5'-biotin-TEG r(UGGAA)$_9$ was immobilized to the surface under the following conditions: 200 nM repeat RNA in 10 mM HEPES (pH 7.4), 500 mM NaCl. Amount of r(UGGAA)$_9$ immobilized on the chip surface was 476 response units (RU). SPR analysis for the binding of non-hit compounds to the r(UGGAA)$_9$-immobilized surface was performed using a BIAcore T200 SPR system (GE Healthcare) under the following condition: 10 μM compounds in HBS-EP+ buffer (GE Healthcare) containing 5% DMSO. The binding of SMN-C5, risdiplam, CM-D1, and CM-D2 were analyzed in sigle-cyle mode. These ligands were sequentially injected at concentrations of 1.25, 2.5, 5, 10, and 20 μM.

Synthesis of NBD-NCD

A mixture of NCD-linker[1,2] (20 mg, 31 μmol), NBD-COOH (15 mg, 50 μmol), 1-ethyl-3-(3-dimethylaminopropyl)carbodiimide hydrochloride (10 mg, 50 μmol), and 1-hydroxybenzotriazole (8 mg, 50 μmol) in DMF (2 mL) was stirred overnight at room temperature. The solvent was removed *in vacuo*. The resulting mixture was dissolved in chloroform and washed with sat. $NaHCO_3$ aq. and brine. The organic layer was dried over $MgSO_4$ and evaporated to dryness. The crude product was purified by silica gel chromatography to give NBD-NCD (13 mg, 46%). ^{1}H NMR (CD_3OD, 600 MHz) δ 8.36 (d, 1 H, J = 7.8 Hz), 8.13–8.08 (m, 4 H), 8.04 (d, 2 H, J = 7.8 Hz), 7.27 (d, 2 H, J = 8.4 Hz), 6.18 (d, 1 H, J = 8.4 Hz), 4.27 (t, 4 H, J = 6.6 Hz), 3.42 (br, 2 H), 3.23 (t, 2 H, J = 6.6 Hz), 3.16 (t, 2 H, J = 7.2 Hz), 2.66 (s, 6H), 2.62 (t, 4 H, J = 7.2 Hz), 2.52 (t, 2 H, J = 7.2 Hz), 2.21–2.17 (m, 4 H), 1.91 (quin, 4 H, J = 6.6 Hz), 1.78–1.69 (m, 6H), 1.66 (quin, 2 H, J = 7.2 Hz), 1.42 (quin, 2 H, J = 7.2 Hz); ^{13}C NMR (CD_3OD, 150 MHz) δ 176.0, 175.4, 163.9, 155.8, 155.4, 155.3, 146.4, 145.7, 145.4, 140.0, 138.6, 138.4, 122.8, 122.3, 119.2, 114.2, 99.5, 64.9, 52.7, 51.3, 44.5, 39.9, 38.9, 36.9, 34.5, 28.9, 27.8, 27.6, 27.5, 26.9, 26.5, 25.0

HRMS (ESI) m/z: calcd. for $[C_{49}H_{55}N_{13}O_9+H]^+$ 922.4318; found 922.4320.

Reference

1. Nakatani, K., He, H., Uno, S, Yamamoto T., and Dohno, C. *Current Protocols in Nucleic Acid Chemistry.*, 2008, Unit 8.6.1–8.6.21.
2. Takashima, Y., Murata, A., Iida, K., Sugai, A., Hagiwara, M., Nakatani, K. *ACS Chem. Biol.*, 2022, **17**, 2817–2827.

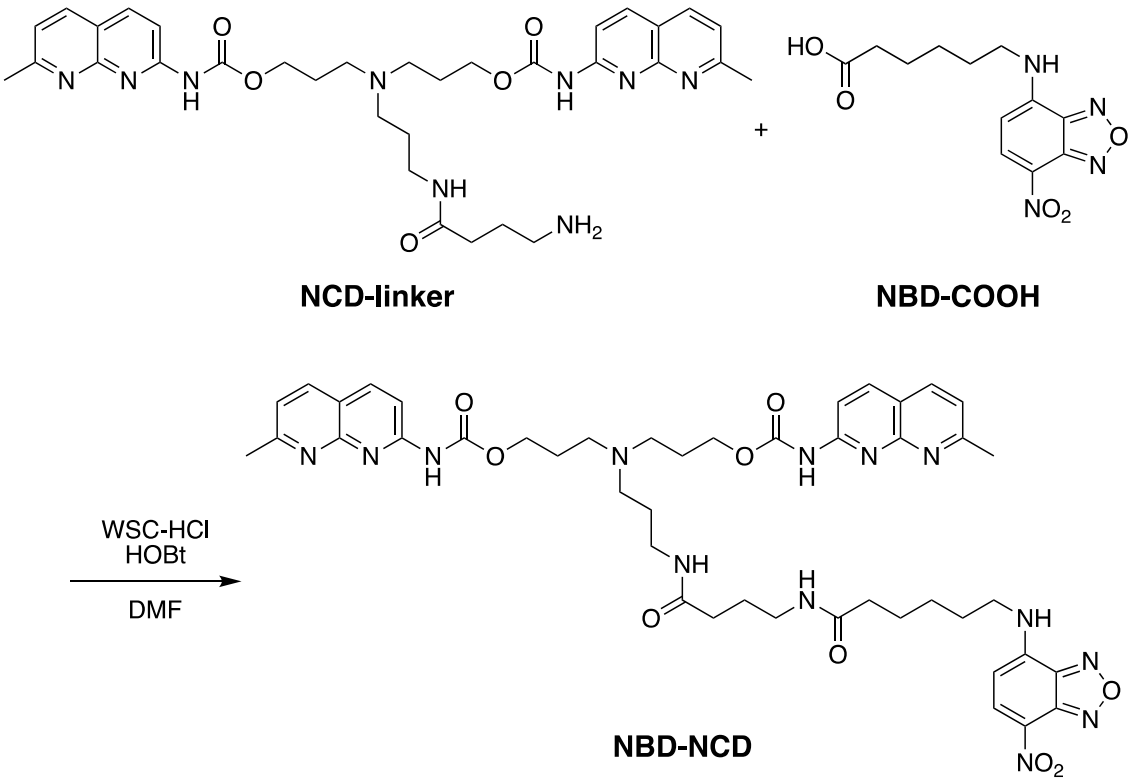

Scheme S1. Synthesis of NBD-NCD

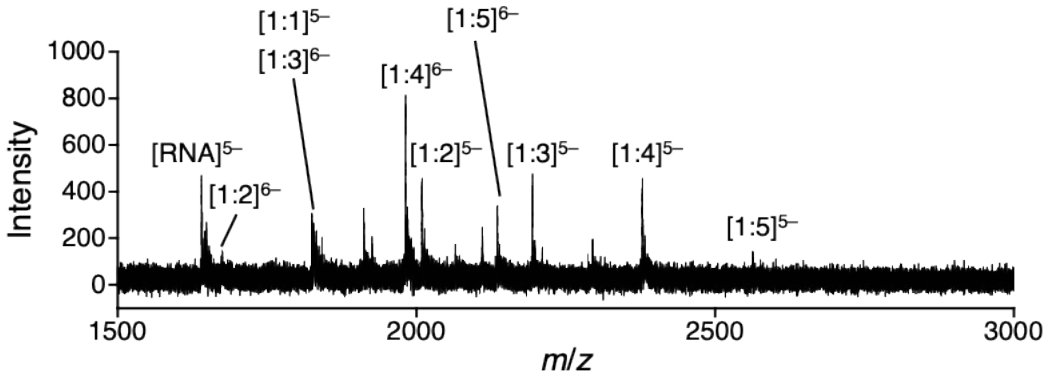

Figure S1. CSI-TOF-MS spectrum of 10 μM r(UGGAA)$_5$ in the presence of 50 μM NBD-NCD.

Table S1. *m*/*z* values of the complexes of r(UGGAA)$_5$ with NBD-NCD[a]

Ion species	*m*/*z* calc.	*m*/*z* found
$[RNA]^{4-}$	2051.28	2051.24
$[RNA]^{5-}$	1640.82	1640.85
$[RNA–NBD\text{-}NCD]^{5-}$ ($[1:1]^{5-}$)	1825.11	1825.14
$[RNA–2NBD\text{-}NCD]^{5-}$ ($[1:2]^{5-}$)	2009.39	2009.41
$[RNA–2NBD\text{-}NCD]^{6-}$ ($[1:2]^{6-}$)	1674.33	1674.35
$[RNA–3NBD\text{-}NCD]^{5-}$ ($[1:3]^{5-}$)	2193.68	2193.76
$[RNA–3NBD\text{-}NCD]^{6-}$ ($[1:3]^{6-}$)	1827.90	1828.03
$[RNA–4NBD\text{-}NCD]^{5-}$ ($[1:4]^{5-}$)	2377.96	2378.30
$[RNA–4NBD\text{-}NCD]^{6-}$ ($[1:4]^{6-}$)	1981.47	1981.47
$[RNA–5NBD\text{-}NCD]^{5-}$ ($[1:5]^{5-}$)	2562.25	2562.62
$[RNA–5NBD\text{-}NCD]^{6-}$ ($[1:5]^{6-}$)	2135.04	2135.44

[a] *m*/*z* values were observed in CSI-TOF-MS spectra of 10 μM r(UGGAA)$_5$ in the absence and presence of 50–100 μM NBD-NCD.

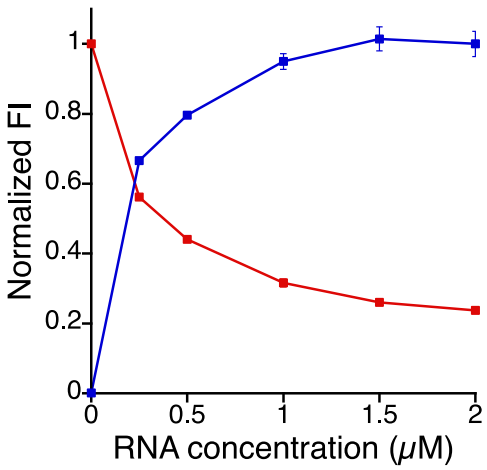

Figure S2. Plots of RNA concentration versus normalized FI of X2S (red) and TO-PRO-1 (blue) in the presence of r(UGGAA)$_9$ at concentrations of 0.25, 0.5, 1, 1.5, and 2 μM. The concentration of fluorescence indicators was 1 μM. The FI of X2S in the presence of RNA was normalized with that of only X2S. The FI of TO-PRO-1 was normalized with that in the presence of 2 μM RNA.

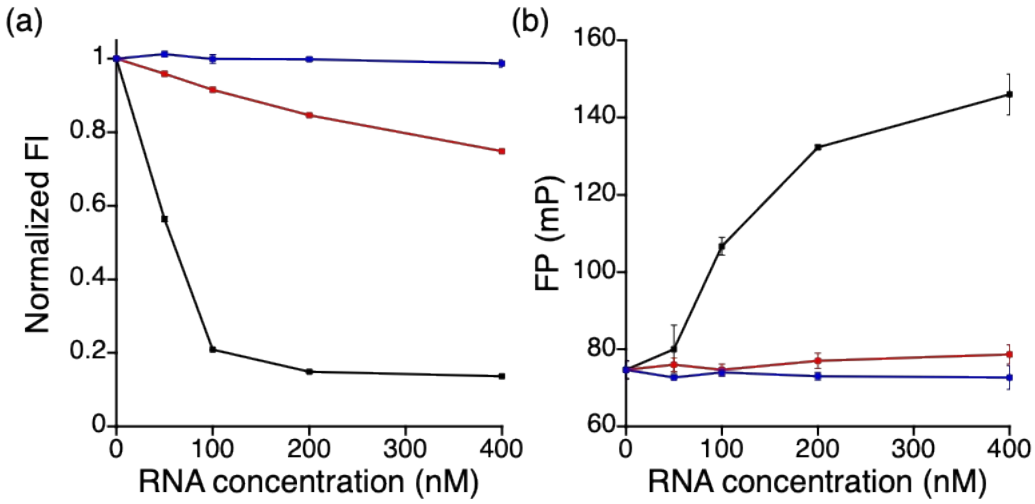

Figure S3. Plots of RNA concentration versus (a) normalized FI and (b) FP of 1 μM NBD-NCD in the presence of r(UGGAA)$_9$ (black), r(UAGAA)$_9$ (red), and r(UAAAA)$_9$ (blue) at concentrations of 50, 100, 200, and 400 nM.

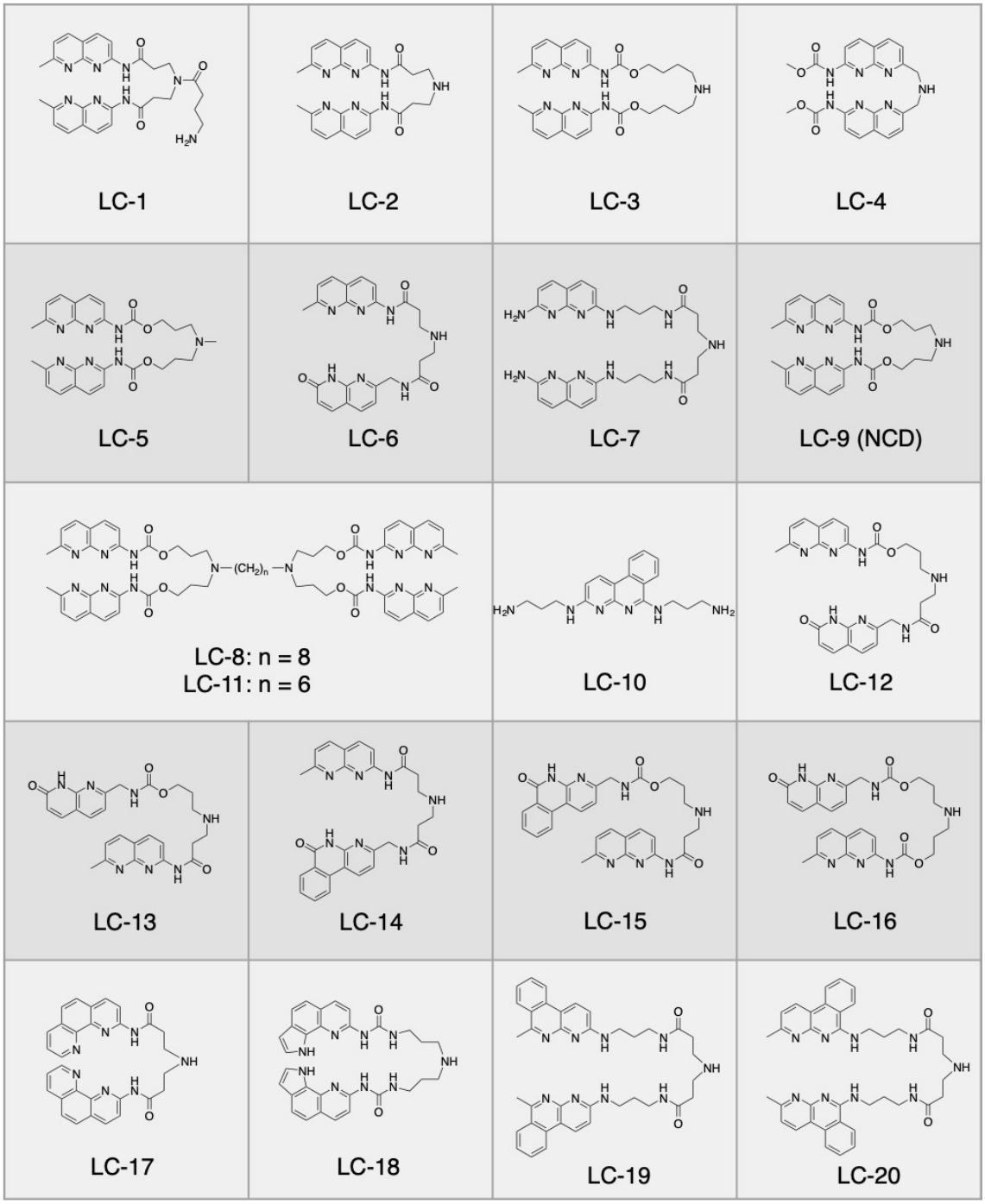

Figure S4. Chemical structures of LC-1~LC-20.

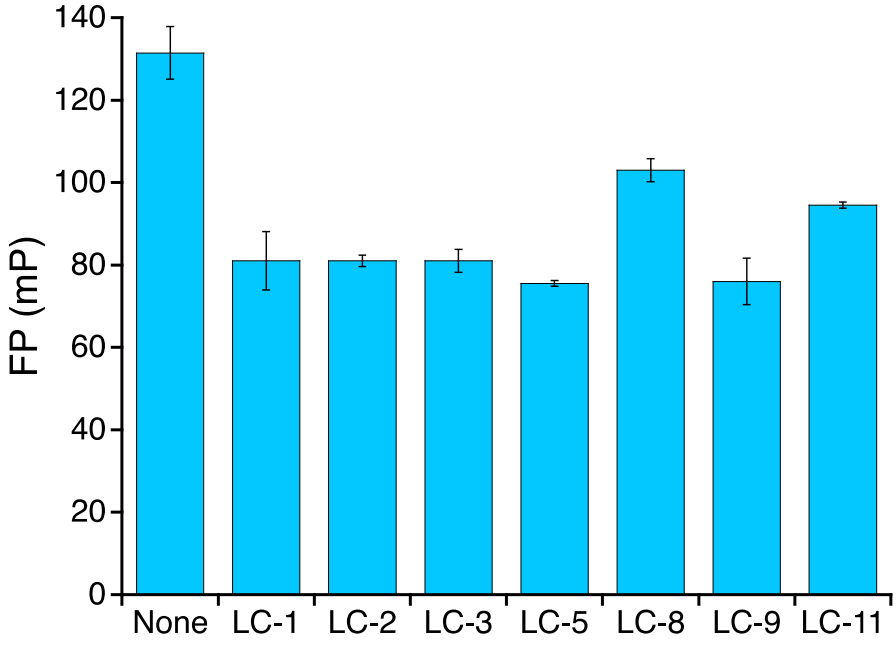

Figure S5. Fluorescence polarization of 1 μM NBD-NCD with 200 nM r(UGGAA)$_9$ in the absence and presence of 10 μM LC-1, LC-2, LC-3, LC-5, LC-8, LC-9, and LC-11.

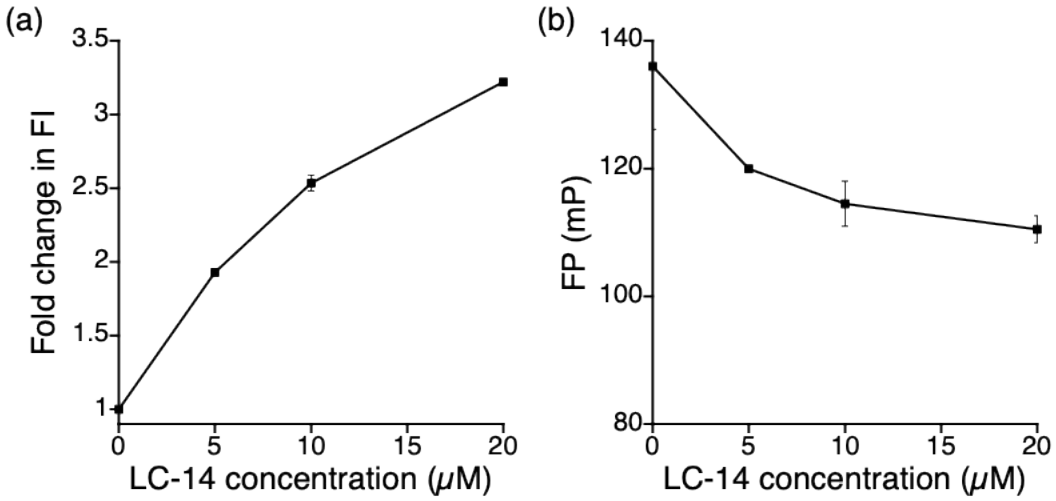

Figure S6. Plots of LC-14 concentration versus (a) fold change in FI and (b) FP of 1 μM NBD-NCD with 200 nM r(UGGAA)$_9$ in the presence of LC-14 at concentrations of 5, 10, and 20 μM.

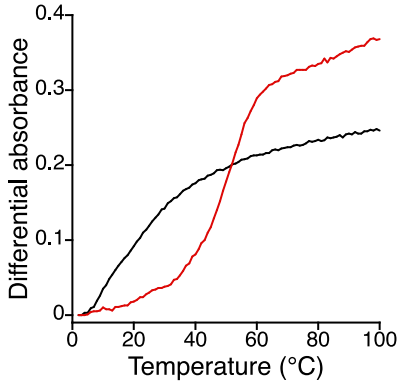

Figure S7. UV melting curves of r(UGGAA)$_9$ in the absence (black) and presence of LC-14 (red). RNA and ligand concentrations were 2 μM and 40 μM, respectively.

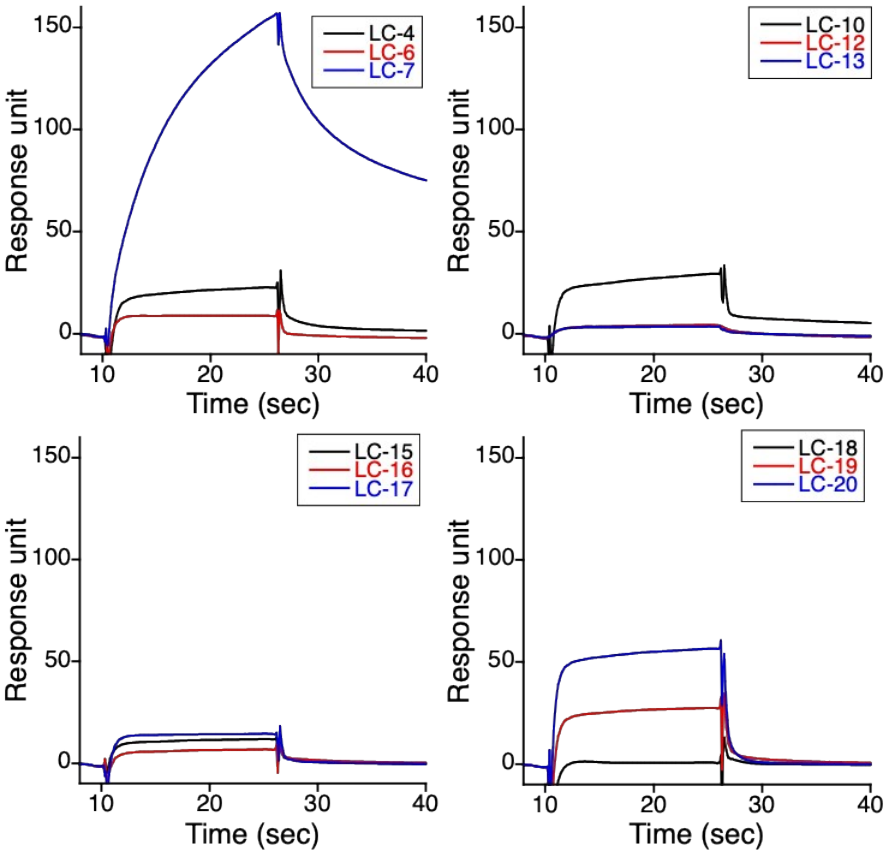

Figure S8. SPR analysis of the binding of non-hit compounds to r(UGGAA)$_9$-immobilized surface. Compound concentration was 10 μM. The amount of 5'-biotin-labelled r(UGGAA)$_9$ immobilized on the SA sensor chip was 476 RU.

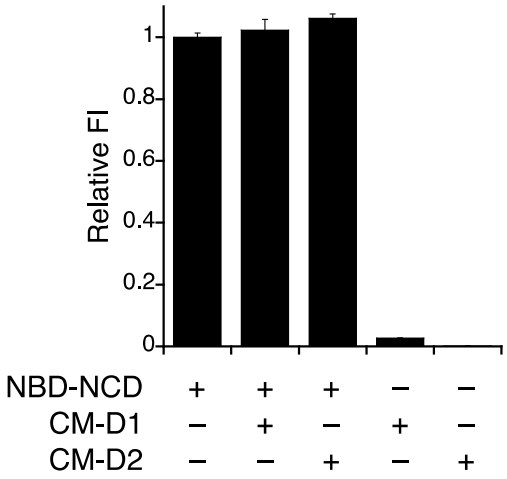

Figure S9. Relative fluorescence intensity (FI) of 1 μM NBD-NCD in the absence and presence of 10 μM CM-D1 or CM-D2. The FI of each sample was measured with 510 nm excitation and 560 nm emission.

Discussion: CM-D1 and DM-D2 did not significantly affect the fluorescence of NBD-NCD. This result suggested that the fluorescence of CM-D1 and CM-D2 do not interfere with the FID assay using NBD-NCD.

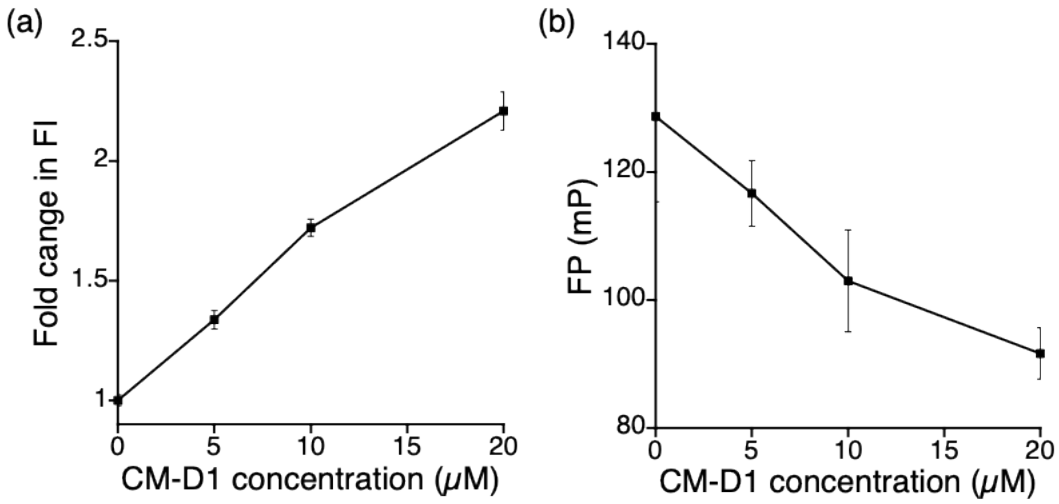

Figure S10. Plots of CM-D1 concentration versus (a) fold change in FI and (b) FP of 1 μM NBD-NCD with 200 nM r(UGGAA)$_9$ in the presence of CM-D1 at concentrations of 5, 10, and 20 μM.

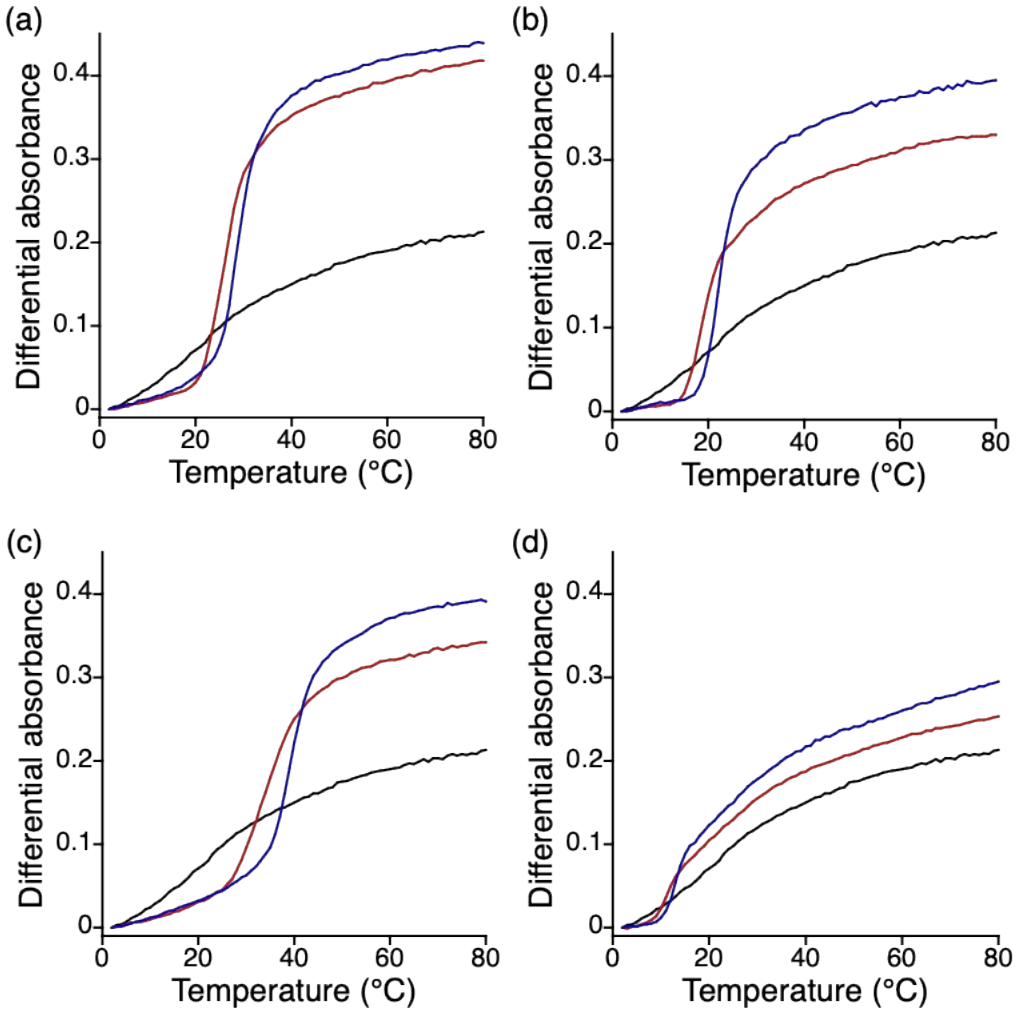

Figure S11. UV melting curves of r(UGGAA)$_9$ in the absence (black) and presence of (a) SMN-C5, (b) risdiplam, (c) CM-D1, or (d) CM-D2. RNA and ligand concentrations were 2 μM and 20 (red) or 40 μM (blue), respectively.

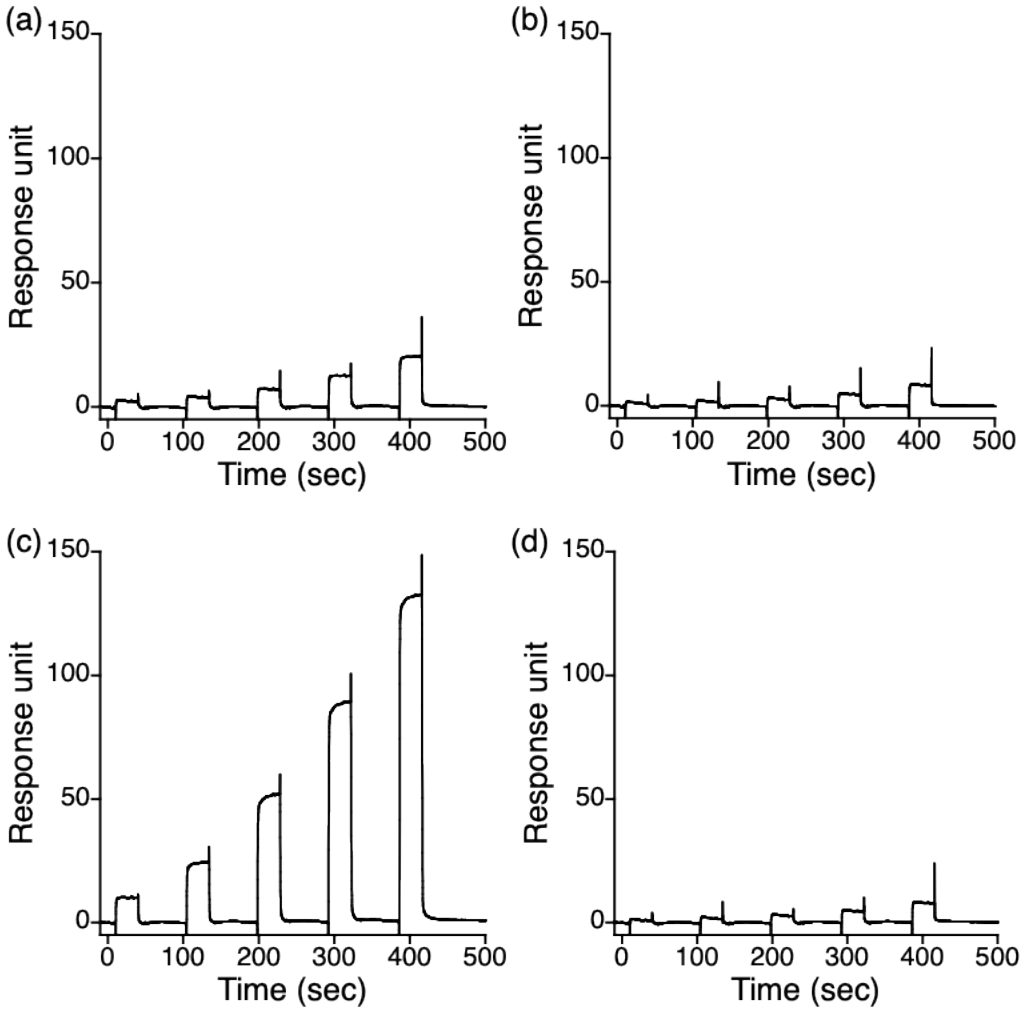

Figure S12. SPR analysis of the binding of (a) SMN-C5, (b) risdiplam, (c) CM-D1, and (d) CM-D2 to r(UGGAA)$_9$. The ligand was sequentially added at 1.25, 2.5, 5, 10, and 20 μM.

^{1}H NMR of NBD-NCD

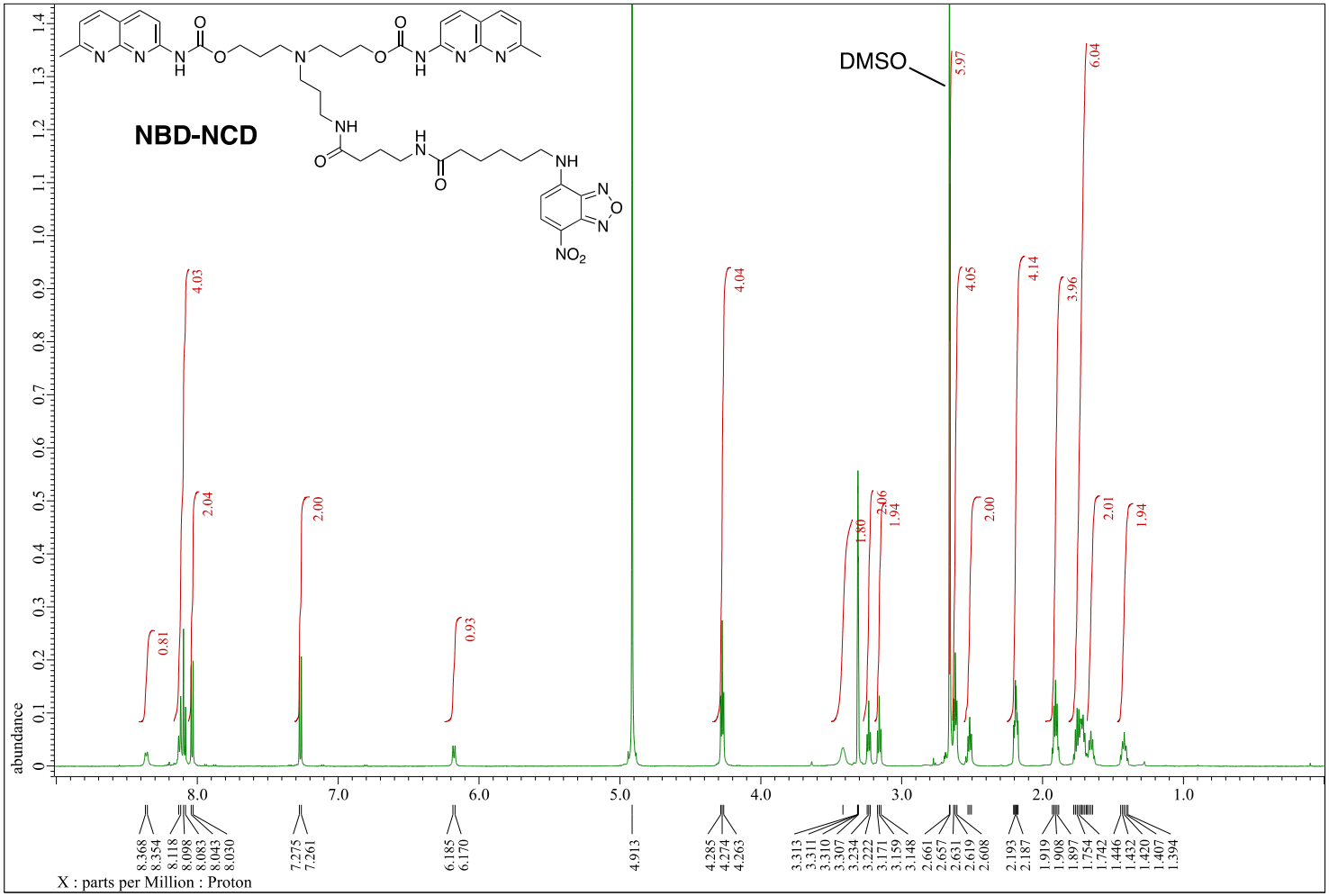

^{13}C NMR of NBD-NCD